Thermal / Stress Finite Element Analysis Applied To The Design and Packaging of a Vaporizing Liquid Microthruster

Andrew P. Wallace

Jet Propulsion Laboratory, Reliability Technology Group,
M/S 301-456, 4800 Oak Grove Dr., Pasadena, CA, 91109;
wallace@oak.jpl.nasa.gov

Abstract

The Jet Propulsion Laboratory is currently under NASA contract to develop a vaporizing liquid microthruster. An essential part of this product development is to estimate the power loss to the environment, which is critical due to the requirements of new low power microspacecraft. The current design utilizes a "thermal choke" to enhance thermal insulation. This choke, as part of the vaporizing chamber, is subjected to pressure from the fluid. Due to this pressure, stress analysis models are required to ensure reliability under loading. A finite element sensitivity analysis was used to compare the effectiveness of the thermal choke to the ability to withstand the fluid pressure. Furthermore, the microthruster consists of various materials either deposited or bonded together in the manufacturing of the actual thruster and packaging. Finite element analysis was used to characterize the temperature gradient throughout these materials. This paper presents all of the finite element analyses used up to this stage of the microthruster design.

1. Introduction

One of the key challenges in the development of microspacecraft in the 1 to 10 kg class is propulsion due to unique system requirements. As examples, propulsion systems will require lower leak rates due to the reduction in propellant quantities, thrust and impulse bits must decrease in order to provide accurate attitude control, and a high specific impulse is required for missions with large delta-v requirements.[1] One of the thrusters being developed to address some of these challenges is the vaporizing liquid microthruster (VLM).

As part of the VLM development, the Reliability Technology Group is utilizing the Defect Detection and Prevention (DDP) Methodology[2] in order to address reliability issues during the design process. As part of the DDP implementation, finite element analysis (FEA) is one tool used to evaluate the criticality of particular failure modes. There are both system level and device level failure modes; for instance, failing to meet the stringent power requirements of microspacecraft is a failure mode in the general sense, while overstress of the silicon bridge due to fluid pressure loading is a specific failure mechanism.

The microthruster has many challenging aspects; for instance, numerous manufacturing steps are required as there are a number of layers and adjoining materials. However, the work presented here does not address the issues of microfabrication, but rather, it provides insight into the geometry design, material selection, and the environmental constraints.

2. Vaporizing Liquid Microthruster (VLM) Geometry

The geometry for the VLM is shown in Figure 1. Fluid entering the chamber is vaporized by thermal input from the electric heaters; the vaporized fluid then passes through the exit nozzle at a much higher velocity.[3] Preliminary microthruster work utilizes water as the working fluid. Other possible fluids include ammonia and hydrazine, which will be explored at a later date.

Figure 1: Schematic Diagram Of Vaporizing Liquid Microthruster

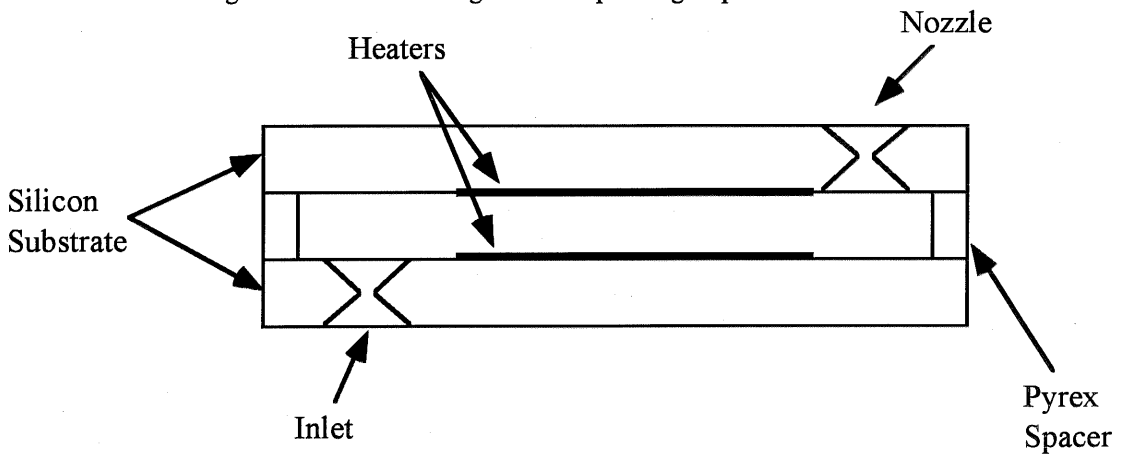

The microthruster design is symmetrical about the central axis of the vaporizing chamber. The chamber has a cross sectional area of 500 microns by 500 microns, and a length of 5000 microns. The top and bottom substrates (where the nozzles are etched into) of the vaporizing chamber are silicon. A cross-sectional side view of the bottom substrate is shown in Figure 2; Figure 3 is a 3D view of the bottom substrate. The fluid travels just over the center of the bridge; this bridge configuration was constructed to aid the thermal insulation of the thruster. The silicon substrate cut-out was manufactured by etching <100> silicon in KOH, which forces both the nozzle and bridge angles to be 54.7°.[4] Due to the relatively high thermal conductivity of silicon, the bridge only provides limited thermal insulation. However, since the nozzle is etched into the silicon, implementation of the silicon bridge does not provide a significant increase in the number of manufacturing steps, as it can be part of the same etching processes.

Furthermore, the same bridge configuration will be used for an additional thruster design as well. The substrate will be inverted, and a Pyrex cover will be directly bonded to the substrate giving a simplified microthruster design, with only one heater.

Heaters exist on both the top and bottom surfaces of the thruster chamber; the electric heater material is n-doped poly-silicon which is deposited on the silicon substrate. The side chamber walls are Pyrex. A single piece of Pyrex with a hole in the center is anodic bonded to the silicon substrates. The Pyrex was chosen with a CTE closely matching that of silicon.

Due to the high temperatures required to vaporize the thruster fluid, temperature losses through the substrate and package may require large power inputs to enable fluid vaporization. A number of steps are underway to ensure acceptable thermal insulation, notably: the heater to substrate interface layer, the substrate to package insulation, and the bridge geometry of the substrate.

Figure 2: VLM Substrate Model -- 2D Cross-Section (underneath heater)

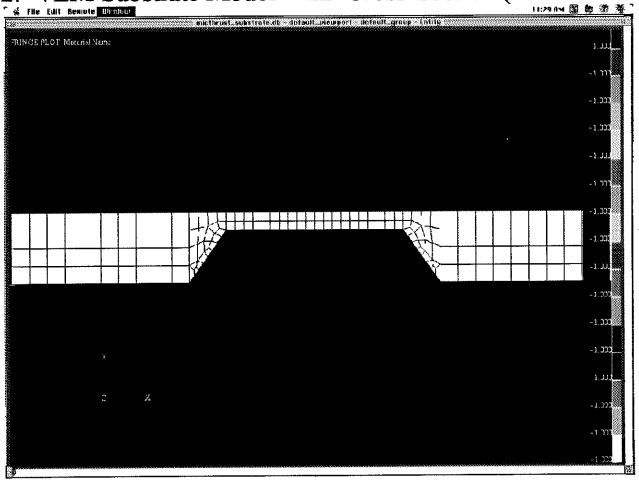

3. Need For Thermal / Stress Finite Element Analysis

As stated earlier, the bridge design was implemented to serve as a thermal choke to limit heat loss through the package. Also, the temperature gradients in the VLM will induce stresses due to coefficient of thermal expansion (CTE) mismatches. Furthermore, the silicon bridge will be subjected to pressure loading from the fluid in the vaporizing chamber. The VLM, therefore, requires thermal, stress, and thermally induced stress analysis. While some of these areas may be investigated solely by hand calculations, finite element analysis yields the advantage, that all of these areas may be investigated by utilizing a single finite element analysis model. The current model only address the thermal requirements of the heater and the silicon bridge strength under fluid pressure loading. Patran® was used to generate the model geometry and finite element meshes. The solvers P3 Thermal® and AdvancedFEA® were used for thermal and stress analysis, respectively[5].

4. Finite Element Model Development

All model geometry was generated in units of microns to avoid meshing errors due to numerical inaccuracies caused by the relatively small dimensions of the microthruster. A micron to meter conversion was then used by Patran® during creation of the input deck. Figure 4 displays an analysis sanity check used to compare a simple FEA model against a hand calculation. The results correspond exactly to that of a hand calculation using the basic thermal conduction equation: $q = (T_2 - T_1)/(l/kA)$, where q is the heat input, T_2 and T_1 are temperatures for the surfaces in question, and l/kA is the thermal resistance; l, k, A are defined as length, thermal conductivity and surface area, respectively[6]. While this first analysis step may seem overly simplistic, it is essential to be able to at least bound finite element analysis results with hand calculations in order to establish confidence in the model, material property definitions, and the FEA package in use. All material properties used in the analyses are recorded in Table 1.

Figure 5 includes the additional thermal resistances which are in parallel due to the side thickness of the substrate. Identical boundary and load conditions were used. The results of this analysis are recorded in Section 6. Due to the high thermal conductivity of silicon, it was desired to increase the effective thermal resistance of the silicon substrate. This was done by implementation of the bridge configuration as shown in Figure 2 and Figure 3, which are 2D and 3D representations of the substrate, respectively. The fluid travels over the top of the bridge surface. The heater power is applied on a per node basis. The power applied to each node (for a 2D model) = Total Heater Power/ (# of Elements * Heater Length in meters). The heat applied to each of the heater boundary nodes is one half this amount in order to provide a uniform heat input across the entire heater surface. The 3D model of this will be used for a future advection analysis, where the 1D advection elements are placed on the heater elements (described in the Future Work Section).

The current analysis assumes perfect symmetry about the center axis of the chamber; while this is true for the thruster geometry, the assumption breaks down when investigating the effects of packaging and environmental loading. For instance, the fluid as a liquid, upon entering the thruster, serves as a heat sink, but the exiting fluid at the top of the thruster has been vaporized and is at a much higher temperature. Furthermore, the packaging configuration is different on the top and bottom of the VLM, and the package boundary conditions are different as well. The package bottom is connected directly to the spacecraft, while the top package surface is coupled by radiation to deep space. However, despite these conditions, the current FEA assumes symmetrical conditions.

All of the results reported here are results of 2D FEA models. Due to the chamber aspect ratio, the chamber is assumed to be sufficiently long as compared to the width to assume a 2D heat transfer problem.

Detailed spreadsheet calculations for a steady state analysis of the fluid vaporization were carried out by Blandino and Mueller [16]. These calculations estimate that ~2 Watts are required to vaporize the fluid. The finite element analysis presented here is used to estimate the power required to keep the chamber surface temperature at the appropriate level based on loss to the environment (this is also the power required for a pre-warm). By adding the results of the FEA (Section 8) to those in reference 16, the heater power required for steady state conditions may be estimated, and the heater sizing can be done based on the polysilicon resistivity and the voltage/current available.

Figure 3: 3D Model VLM Substrate Generated For Advection Analysis

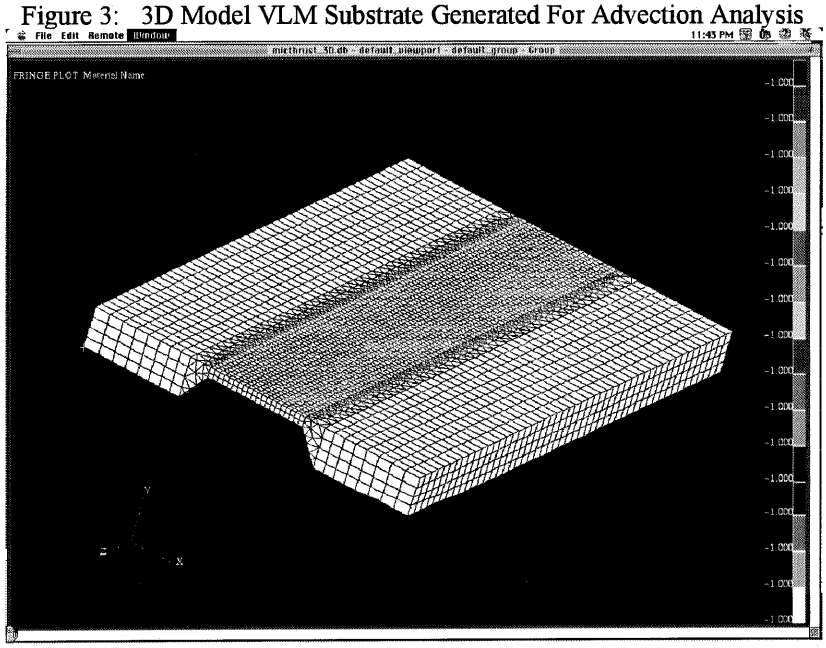

Figure 4: Analysis Sanity Check

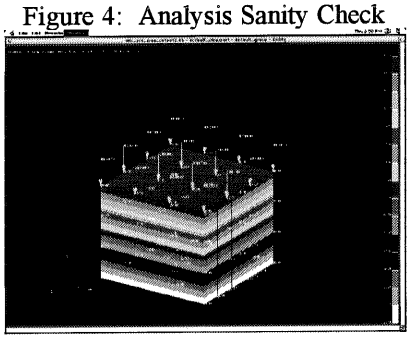

Figure 5: 2D Simple Substrate Model

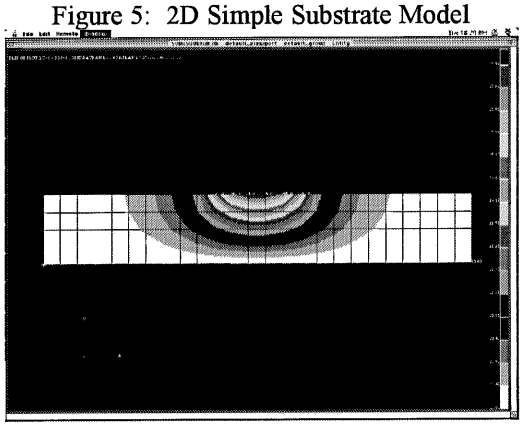

5. Material Properties

Material property definition is often one of the most challenging aspects of any analysis. In the current problem, the geometries are large on a MEMS (Micro-electro-mechanical Systems) scale. Thus, bulk material properties are used for all analyses. Furthermore, silicon is a cubic crystal, and an anisotropic elastic description should be used. The crystal axes, ([100],[010],[001]), are the base directions for elastic constants for {100} wafers as is the case here[7]. However, for simplicity, the Young's modulus defined in reference 8 will be used. Furthermore, the strength properties are functions of orientation as well, which is often not reported in literature; values for silicon flexural strength ranged from 62 to 580 MPa [10]. In this analysis the worst case value was used to be conservative. Also, the value of thermal conductivity for the epoxy was estimated from various epoxies in reference 6, as it was not reported in the manufacturer's data sheet.

Table 1: Material Definitions Used In Thermal / Stress Finite Element Analysis
Note: [XX] and [XX] are reference numbers

Material	Th Con (W/m*K)	Density (kg/m^3)	Specific Heat (J/kg*K)	Modulus of Elasticity (GPa)	CTE (ppm/°C)	Poisson's Ratio
silicon dioxide	1.4 [8]	2170 to 2660 [9]	745	66 [8]	.5 [8]	.3 [8]
silicon nitride	35 [8]	2400 [10]; 3440 [9]	627 [11]	314 [8]	3.2 [8]	.3 [8]
silicon	83.7 [11]; 120 [8]; 153 [12]	2330 [10]	712 [10]	120 [8]	2.6 [8]	.28 [8]
epoxy[13]	10	–	–	20.6	63 (< 106°C)	–
polyimide	.517 [11]	1910 [11]	1130 [11]	27.2 [12]	41 [11]	–
kovar [10]	16	8360	439	138	5.87	–

6. Bridge Performance Analysis Results

As previously discussed, the silicon bridge is subjected to both thermal and pressure constraints. It is desired to manufacture the bridge to be as thin and wide as possible to enhance the performance of the thermal choke, but these same parameters inversely affect the performance of the bridge under pressure loading. Therefore, the trade-offs between the thermal resistance and bridge strength were investigated.

It is important to note that the 20°C boundary condition, the amount of heat input (10 W), and the resultant maximum temperature are unrealistic values. These were used to determine a relative effectiveness of the thermal resistance (Rth) compared to strength performance. The equivalent thermal resistance of the structure was estimated to be the heat input / (max temp - 20°C).

The 1000 micron width and 100 micron thickness bridge model had a maximum stress of 8 MPa with a 50 psi fluid pressure load. This configuration was selected primarily due to the relatively low stress incurred under pressure loading, while providing some increase in thermal resistance.

Table 1: Thermal Resistance To Strength Comparison For Silicon VLM Substrate

Rth (°C/W)	Max Stress @ 50 psi	Case
~1.0	N/A	1D Heat Conduction (no heat spreading) (Fig 3)
.7	N/A	With heat spread; no substrate cut out (Fig 4)
3.8	8 MPa	Bridge config. -- 1000 micron width; 100 micron thickness (Fig 5)
2.8		Bridge config. -- 700 micron width; 100 micron thickness
6.9	59 MPa	Bridge config. -- 1000 micron width; 50 micron thickness

Figure 6: Thermal Model With 100 micron Thick Wall and 1000 micron Wide Channel

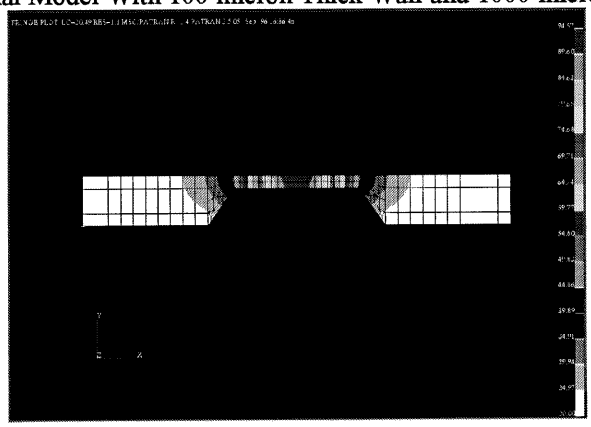

Figure 7: Stress Analysis of 50 micron Thick Wall and 1000 micron Wide Channel

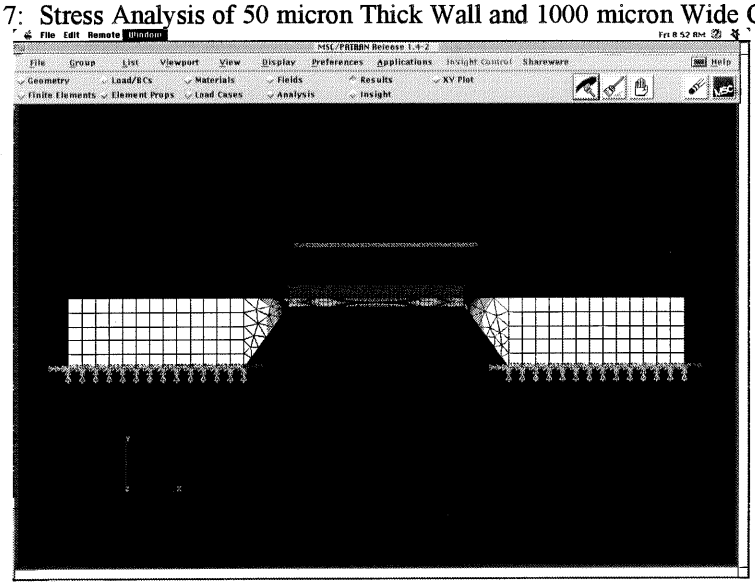

7. Insulative Layer Addition

The next step in attempting to increase the thermal insulation of the thruster chamber is the addition of an insulative layer between the silicon substrate and the polysilicon heater. Both silicon nitride and silicon dioxide layers were analyzed. However, achieving layer thickness much above 3 microns is impractical due to the time required by the microfabrication processes. For simplicity (which in this case is conservative), the contact resistances were assumed to be neglibile between the heater, insulative layer, and the silicon substrate.

The silicon substrate bridge is composed of elements that are 50 microns by 50 microns. To properly align the insulative layer element it must have dimensions of 3 microns by 50 microns. This poor of an aspect ratio may have an impact on results by introducing numerical inaccuracies. To gain insight into this problem a simple thermal model (Figure 8) was developed and compared to a hand calculation. The 1D FEA analysis and the hand calculation (1D conduction equation) compared exactly. From this, the thermal analysis using these element aspect ratios was determined to be acceptable. However, the errors induced by the aspect ratio on the thermal stress analysis are not understood.

Thermal analyses were performed on the substrate with the insulative layer for a 10W input and a 60°C boundary condition. At first, it appears the insulative layer produces a relatively significant saving by producing a temperature gradient of nearly 10°C. However, the 60°C boundary condition is shown to be much too low in accordance with the results from the section below. Once the entire packaging is considered, the heat/substrate interface layer is shown to provide limited insulation, approximatly 3°C drop using a SiO2 insulative layer. The drop is significantly less when using SiN due its much higher thermal conductivity.

Figure 8: Model Used For Error Check With Poor Element Aspect Ratios

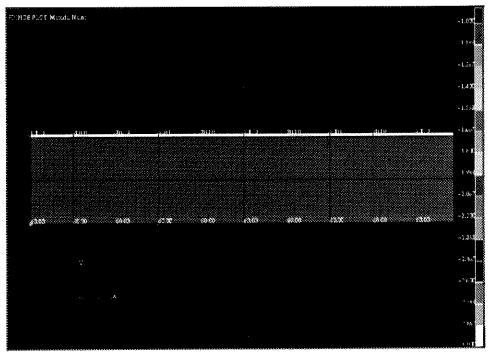

8. Microthruster Packaging

The microthruster is epoxy bonded to a traditional IC package. The package provides a mechanical interface to the fluid inlet, thermal insulation, and electrical interconnection for heater power. After the proof of concept has been completed, future packages may include the propulsion control electronics and temperature monitoring instrumentation.

A hole is drilled through the bottom of the package underneath the inlet nozzle. Precise alignment is not critical providing the hole in the package is large enough to encompass the microthruster inlet. A bose is then attached to the bottom of the package, and the fluid supply tube is soldered into a hole in the bose. The first design iteration includes a polyimide interface layer to provide thermal insulation. The accompanying finite element model is shown in Figure 9. The bottom layer is the Kovar package, and the interface layers are the epoxy bonds. Both the polyimide and Kovar sections were assumed to be 1/16 inch (1587.5 micron) thick, and the epoxy bonds were assumed to be 5 mil (127 micron) thick.

Figure 10 shows the results of the thermal analysis of the structure with the package for a 1 Watt heater input and a 20°C boundary condition applied to the bottom of the Kovar package; the maxiumum temperature over the bridge was shown to be 108°C. This analysis yields a number of interesting results. First, since much lower power is required to raise the thruster to the appropriate temperature, due to the added insulation, there is a much smaller temperature drop across the silicon dioxide heater to substrate interface layer. The extra manufacturing steps associated with the insulation manufacturing only add a few degrees of insulation. Up to this point, all thermal analyses used 153 W/mK for the silicon thermal conductivity; due to this, there is very little temperature gradient across the silicon substrate. Thus, the temperature at the epoxy will reach greater than 100°C, which approaches the glass transition temperature of the first epoxy selected. New epoxy selection is currently underway.

Figure 11 is a repeat of the thermal analysis of Figure 10, with the substitution of 83.7 W/mK for the thermal conductivity of silicon. The bridge in this scenario is more effective, and the maximum temperature increases by over 40°C to 150°C with the same boundary conditions and a 1W heat input.

It should be noted that while the first design iteration includes polyimide as an insulative layer; it will most probably not be use in the final design due to its moisture absorption properties[14]. Once the package boundary conditions have been analyzed more fully, either a more appropriate insulator will be found or the thruster will be bonded directly to a ceramic package.

Figure 9: Finite Element Model Including Package Insulation Layers

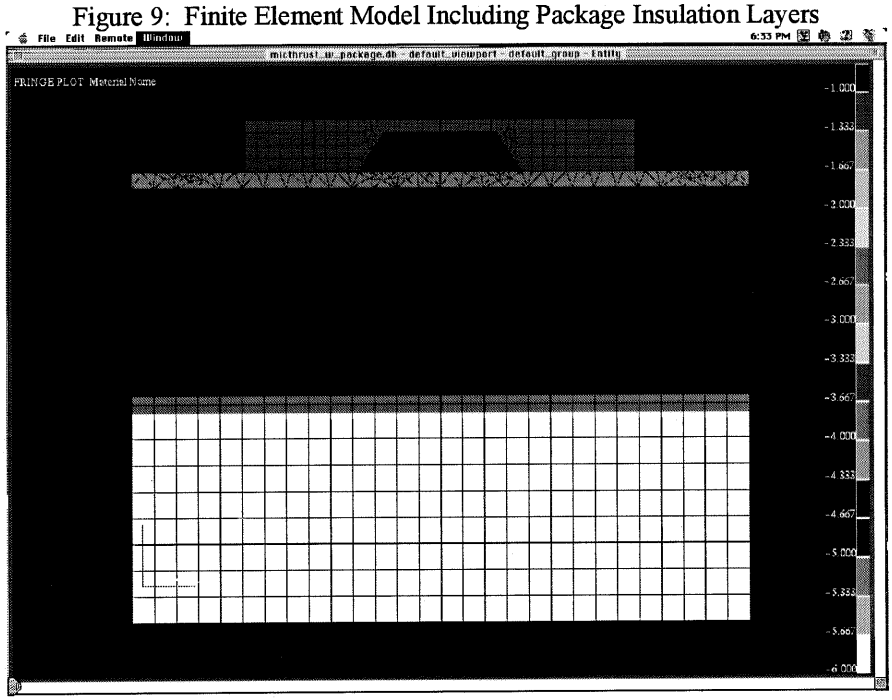

Figure 10: Thermal Analysis: 1 Watt Power Input; Th Con of Si =153 W/mK

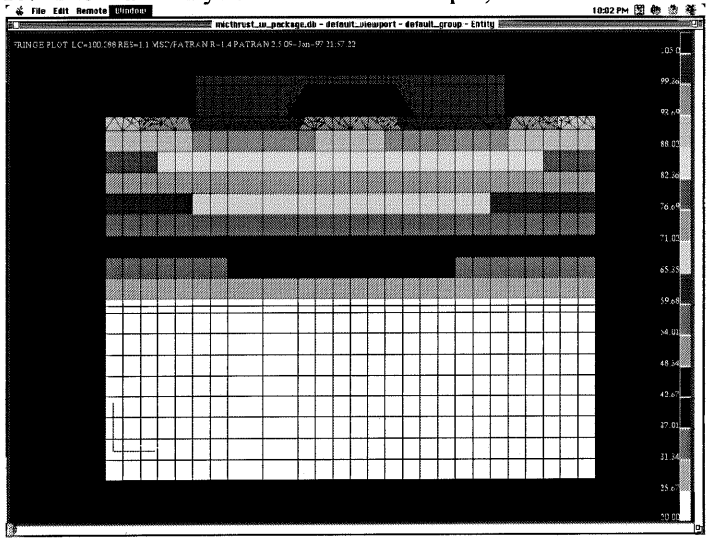

Figure 11: Thermal Gradient: 1 Watt Power Input; Th Con of Si =83.7 W/mK

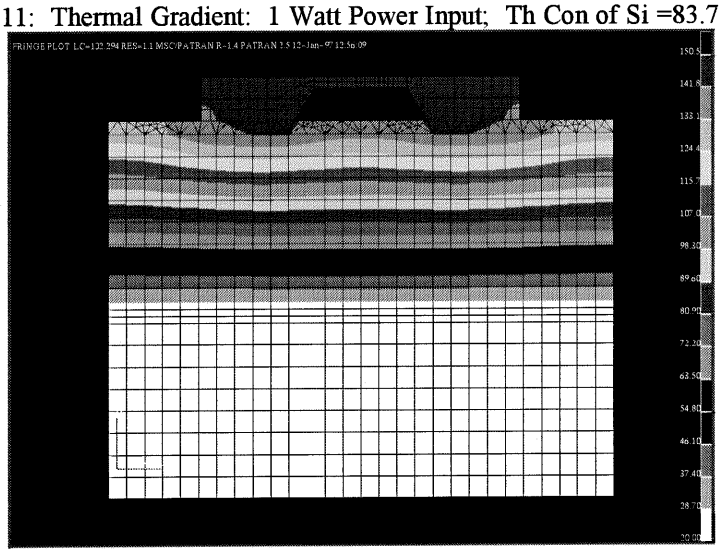

9. Thermal Induced Mechanical Stress

The large temperature gradients that exist within the microthruster and packaging will create stresses at material interfaces due to coefficient of thermal expansion (CTE) mismatches. Furthermore, temperature gradients will cause stresses at interfaces even with materials that have comparable CTE values. Results from thermal analyses may be used to great a temperature field in the finite element model which can later be used as a temperature load for a thermal stress analysis. The results of which are not presented here as the package geometry and material selection is still under evaluation. However, the current bridge model will be directly expanded as the microthruster package design continues.

10. Future Work

The current microthruster will serve as a building block for future analyses. In particular, Pyrex/Silicon bond strength tests are underway, results of which shall be compared to a thermal stress and pressure analysis of this interface. Furthermore, the environmental boundary conditions will be evaluated in greater detail using the existing model. Also, it is hoped to combine all of the previously discussed material with advection analysis to provide a complete model of the microthruster operation. Advection is the heat transfer to a fluid based on the mass flow rate and the fluid specific heat as defined in the Patran® User Manuals[5]. The mass flow rate has been calculated by other methods not discussed here.[15,16] For a

problem with constant specific heat and at constant mass flow rate, the heat input to the fluid is simply $\dot{m}C_p dT$ [17], which is the standard input required by Patran®. However, in the problem at hand, since fluid vaporization is occurring, the specific heat is clearly not constant. The complexities of this analysis will be reported at a later date.

11. Conclusions

The analyses presented here are relatively simple from an academic point of view. However, this problem is an excellent example of how various parameters work against one another, and how finite element analysis may be used as an iterative tool throughout the design process. Furthermore, as design-to-product turn around times must become shorter and shorter, it is essential to develop analyses with reasonable assumptions to provide manufacturing engineers data in a timely manner, which was the case here. The analysis provided data for geometry selection and reliability engineers input to the Defect Detection and Prevention assessment matrix. In addition, the numerous assumptions made have been documented and will allow others to either critique or add to this analysis. This work has estimated the power loss to the environment to enable heater sizing, determined the silicon bridge structure geometry, addressed the effectiveness of heater to substrate interface layer, and it provides a useful tool to be built upon as the design continues.

Acknowledgments

The research described in this paper was conducted by the Jet Propulsion Laboratory, California Institute of Technology, under a contract with the National Aeronautics and Space Administration. The analyses discussed above are a small part of a large team effort. The author wishes to thank the following who have worked together: Juergen Mueller, the microthruster cognizant engineer, who has managed an effective team and did much of the design and manufacturing, Lilac Muller, who did much of the initial microthruster development, John Blandino, who did a considerable portion of the fluid flow analysis, Bill Tang, who actually defined the microfabrication processes as well as provided significant guidance in numerous areas to the entire microthruster team, Russ Lawton, who has coordinated the various inspection activities, Kin Man for his support and guidance as the MDL support task manager, Jim Newell and John Forgrave, who provided support to the finite element model development, Wen Li and Indrani Chakraborty for their many hours spent in the actual manufacturing of the thruster, and Dave Bame and Morgan Parker for their designs in the valving and functional test setup of the vaporizing liquid microthruster.

About the Author

Andrew Wallace received a BS degree in Mechanical Engineering from the California State University, Northridge. He has been employed at the Jet Propulsion Laboratory since 1991. He is currently a member of the Reliability Technology Group, where he manages testing activities of the Reliability Assessment Technology Testing Laboratory. His current areas of research are qualification of electronic assemblies, physics of failure approach to reliability, finite element analysis applied to electronic packaging and MEMS, and thin film material properties.

References:

[1] Mueller, J., *Micro Propulsion Development at JPL*, JPL Internal Document.
[2] Cornford, S. L., Gibbel, M., *Defect Detection and Prevention*, JPL Internal Document
[3] Mueller, J., Leifer, S.D., Muller, L., George, T., *Vaporizing Liquid Micro-Thruster for Microspacecraft*, New Technology Report NPO-1992819530, Office of Technology Utilization, JPL Internal Document, April 24, 1996
[4] Tang, W. C., *Surface Micromachining*, JPL Internal Document, 1996
[5] Patran 3® User Manuals.
[6] Incropera, F. P., **Introduction to Heat Transfer 2nd Ed.**, John Wiley & Sons, 1990.
[7] Johnson, G. C., MEMS Clearinghouse, http://mems.isi.edu/archives/Discussion_Group/1995/43.html, April 13, 1995
[8] Prabhu, A. S., Barker, D. B., Pecht, M. G., *A Thermo-mechanical Fatigue Analysis of High Density Interconnect Vias*, Reliability Technology Biannual Report, December 1994
[9] **Handbook of Chemistry and Physics 58th Edition**, CRC Press, West Palm Beach, Florida, 1977-78
[10] Pecht, M., **Handbook of Electronic Packaging Design,** Marcel Dekker, Inc. New York, 1991
[11] Materials Selector 1989, Materials Engineering, Penton Publishing, December 1988
[12] Dally, J. W., **Packaging of Electronic Systems**, McGraw-Hill
[13] Manufacturer's Data Sheet
[14] Rogers, K., CALCE Annual Review, University of Maryland, Oct. 1996
[15] Muller, L., *Vaporizing Liquid Microthruster*, JPL Internal Document
[16] Blandino, J., Mueller, J., *Heat Requirements of Fluid Vaporization*, JPL Internal Document, 1996
[17] Cengel, Y. A., **Thermodynamics An Engineering Approach**, McGraw-Hill, Inc.,1989